Magnetic resonance imaging of hypoxia in acute stroke: a cross-validation study against FMISO-positron emission tomography

Valable Samuel, Jérôme Toutain, Didier Divoux, Laurent Chazalviel, Aurélien Corroyer-Dulmont, Ararat Chakhoyan, Stéphane Guillouet, Myriam Bernaudin, Emmanuel Barbier, Omar Touzani

Magnetic resonance imaging of hypoxia in acute stroke: a cross-validation study against FMISO-positron emission tomography

Authors: Samuel Valable [a,†], Jérôme Toutain [a,†,*], Didier Divoux [a], Laurent Chazalviel [a], Aurélien Corroyer-Dulmont [a], Ararat Chakhoyan [a], Stéphane Guillouet [b], Myriam Bernaudin [a], Emmanuel L. Barbier [c], Omar Touzani [a]

[a] Normandie-Univ, UNICAEN, CEA, CNRS, GIP CYCERON, ISTCT/CERVOxy group, Caen, France.

[b] Normandie-Univ, UNICAEN, CEA, CNRS, GIP CYCERON, ISTCT/LDM-TEP group, Caen, France

[c] Univ. Grenoble Alpes, Grenoble Institut Neurosciences, Inserm, U1216, Grenoble 38000, France.

[†] Both authors equally contributed to this work

Running title: Imaging of hypoxia with MRI

Words Counts : 4735

Contributorship: the French National Agency for Research *"Investissements d'Avenir"* n° ANR-11-LABEX-0018-01.

Competing interests: nothing to declare.

Key words: hypoxia; FMISO-PET; stroke; MRI; tissue oxygenation

Abstract:

*Corresponding author: E-mail: toutain@cyceron.fr

Acute ischemic stroke results in ischemic core surrounded by a tissue at risk, named the penumbra, which is potentially salvageable. One way to differentiate the tissues is to measure the hypoxia status. The purpose of the study is to correlate the abnormal brain tissue volume derived from magnetic resonance-based imaging of brain oxygen saturation (S_tO_2-MRI) to the [^{18}F]FMISO positron emission tomography (PET) volume for hypoxia imaging validation, and to analyse the ability of S_tO_2-MRI to depict the different hypoxic tissue types in the acute phase of stroke.

In a pertinent model of stroke in the rat, the volume of tissue with decreased S_tO_2-MRI signal and that with increased uptake of [^{18}F]FMISO were equivalent and correlated ($r=0.706$; $p=0.015$). The values of S_tO_2 in the tissue at risk were significantly greater than those quantified in the core of the lesion, and less than those of the healthy tissue (52.3±2.0%; 43.3±1.9% and 67.9±1.4%, respectively). A threshold value of S_tO_2 of ≈60% as the cut-off for the identification of the tissue at risk was calculated. Tissue volumes with reduced S_tO_2-MRI correlated with the final lesion ($r=0.964$, $p<0.0001$).

The findings show that S_tO_2-MRI approach is sensitive for the detection of hypoxia and for the prediction of the final lesion after stroke. Once validated in acute clinical settings, this approach might be used to enhance the stratification of patients for potential therapeutic interventions.

Abbreviations : **S_tO_2-MRI**: magnetic resonance-based imaging of brain oxygen saturation - **[^{18}F]FMISO**: fluorine-18 fluoromisonidazole – **CBF**: cerebral blood flow – **MCAo**: occlusion of the middle cerebral artery – **CT**: computed tomography – **NEX**: number of experiments – **ADC**: apparent diffusion coefficient – **DWI**: diffusion weighted imaging – **PWI**: perfusion weighted imaging – **EPI**: echo planar imaging - **DSC-MRI**: dynamic susceptibility contrast-MRI – **GE**: gradient echo – **fCBV**: fractional cerebral blood volume - **OSEM-2D**: ordered subset expectation

maximization-2D – **TTP**: time to peak – **ROI**: regions of interest - **F_iO_2**: fraction inspired in oxygen – **SD**: standard deviations – **SUV**: standardized uptake value – **ANOVA**: analysis of variance – **ROC**: receiver-operating characteristic – **AUC**: area under the curve

1 – INTRODUCTION

Ever since the seminal work of Astrup and colleagues [1], it is known that acute ischemic stroke results in an irretrievably damaged ischemic core surrounded by a tissue at risk, named the penumbra, which is potentially salvageable. The penumbra is characterized by hypoxia which is the unavoidable consequence of a decrease in cerebral blood flow (CBF) [2,3]. Techniques able to non-invasively map hypoxia are important to obtain insights into the pathological status of the tissue and to possibly select patients for adapted therapeutic interventions [4]. Positron emission tomography (PET) with fluorine-18 fluoromisonidazole ([^{18}F]FMISO) has been defined as the "gold standard" to image hypoxia in stroke subjects and to visualise the ischemic penumbra [2,5-7]. However, [^{18}F]FMISO has a limited initial penetration in areas of low perfusion and a slow accumulation inside hypoxic regions, which hinders its use in the hyper-acute stage of stroke [8]. Moreover, the cumbersome logistics of PET limit the use of [^{18}F]FMISO for emergencies such as stroke. MRI has been proposed as an alternate approach to map the level of brain oxygenation through the assessment of variations of T2* and quantification of cerebral metabolic rates of oxygen [9-11]. Recently, an approach to evaluate brain tissue oxygen saturation (S_tO_2) with MRI was described [12,13]. MRI maps were calculated as a function of the T2* signal after correction of magnetic field inhomogeneities, total blood volume and T2 effects [12,13]. This approach, based on a modified quantitative BOLD (qBOLD) paradigm [14], detects variations in brain oxygenation in both hyperoxic and hypoxic conditions in man and rodents [13, 15-17]. Nonetheless, no formal validation of this approach has been carried out.

The purpose of the present study was to compare the abnormal brain tissue volume derived from S_tO_2-MRI to the [^{18}F]FMISO PET volume for hypoxia imaging validation, and to analyse the

ability of S_tO_2-MRI and [^{18}F]FMISO PET to describe the different hypoxic tissue types in the acute stage of stroke.

2 - METHODS

2.1 - Animals preparation

The experiments were performed on male Sprague-Dawley rats (CERJ, France) weighing 300-350g (12-14 weeks of age). The experimental procedure, summarized in Figure 1, was approved by the Ethics Committee for Animal Research (CENOMEXA N/01-01-12/01/01-15) and carried out in accordance with the EU Directive 2010/63/EU for animal experiments. Rats were kept in conventional housing with access to food and water *ad libitum*. Data are reported according to ARRIVE guidelines. Based on the literature and a power analysis, 12 animals were included in this study.

2.2 - Induction of cerebral ischemia

Rats were anesthetized with isoflurane (2-2.5%) in O_2/N_2O (30%/70%). A permanent brain ischemia was induced by intraluminal occlusion of the middle cerebral artery (MCAo) [18]. Briefly, a nylon filament with a distal cylinder (0.38 mm diameter) was introduced into the lumen of the external carotid artery and was advanced into the internal carotid artery up to the origin of the MCA. Body temperature was maintained at 37.5°C. An analgesic treatment (buprenorphine 0.05mg/kg s.c, Buprecare®) was delivered during the surgery.

2.3 - Positron Emission Tomography

Fifteen minutes after MCAO, the rats underwent an initial MRI examination and thereafter [^{18}F]FMISO was injected (≈86MBq/kg, i.v) and then the rats were awakened. Two hours later, the animals were re-anaesthetized (isoflurane 2%) and positioned in the preclinical PET machine (Siemens-Inveon®, Germany). Subsequently, a CT scan was performed for attenuation correction,

followed by an emission scan session during 20 min. After the accomplishment of the PET session, the rats were transferred to the MRI suite (adjacent to the PET facility) for a multiparametric MRI examination. During all imaging procedures, body temperature and respiratory rate of the animals were monitored.

2.4 - MRI acquisition

Each animal underwent 3 MRI sessions (Figure 1). MRI was conducted on a 7 T preclinical scanner (Pharmascan, PV5.1 Bruker BioSpin MRI, Ettlingen, Germany) with a gradient insert (Model BGA-9S, Bruker) of maximum amplitude 300 mT/m and slew rate 3000 T/m/s, and a cross coil configuration was used (90 mm horizontal volume transmitting coil / 1H receive-only rat brain surface coil (Bruker , Ettlingen, Germany)). Localized high-order shim (MAPshim) based on the B0map was applied. Under anaesthesia (isoflurane 1.5-2%), rats were placed in a stereotaxic head holder in the magnet. The following imaging sequences were completed:

Echo planar imaging (EPI) sequences were performed with a single shot, double sampling k-space coverage with identical bandwidth and geometry.

Diffusion weighted imaging (DWI): EPI-DWI was acquired both at 15 min (before the PET examination) and at 180 min (just after the PET examination) as well as 24 h after the induction of ischemia. The following parameters were employed: resolution=0.3x0.3x1.5mm, FOV=31.5x15x15mm ; TR/TE=3000/46.4 ms; b-values: 0 and 1000 s/mm^2; 30 directions; Number of experiments (NEX) =3; acquisition time: 5min15. Apparent diffusion coefficient (ADC) maps were then generated with PV5.1 software (Bruker, Ettlingen, Germany).

T2-weighted imaging (T2-w): T2-w images were performed at 3h and 24 h after the occlusion with the following parameters: rare factor=8; resolution=0.15x0.15x0.75mm;

FOV=38.4x38.4x15mm; TR/TE=5000/65 ms; NEX=2; 20 adjacent slices with 0.75 mm thickness; zero-filling=1.34 in phase; acquisition time: 4min.

Vascular imaging: Five EPI T2*w (TR=20,000 ms; NEX=3; 50 contiguous slices; resolution=0.3x0.3x0.3mm; FOV=31.5x15x15mm; echo times= 12, 15, 18, 21 and 24 ms; Partial-FT=1.33 in phase) and four EPI T2-w (TR =20,000 ms; NEX=3; 10 contiguous slices; resolution=0.3x0.3x1.5mm; FOV=31.5x15x15mm; echo times= 40, 60, 80 and 100 ms); acquisition time of each scan=1mn; total acquisition time=9mn.

Perfusion with Dynamic Susceptibility Contrast-MRI (DSC-MRI): Gradient-echo (GE) EPI were acquired continuously 15 s before and up to 105 s after a bolus injection of particles of iron oxides (66 µmol/kg, P904®, Guerbet, France) [16]; (TR/TE_{eff}=400/9.17 ms; number of repetitions=300; 10 slices; resolution=0.3x0.3x1.5mm; FOV=31.5x15x15mm; acquisition time =2 min).

Fractional Cerebral Blood Volume (*f*CBV): Immediately after the DSC-MRI acquisition, a second administration of P904® was performed to attain a total dose of 200 µmol/kg and an EPI-T2*w (TE=12 ms) was acquired.

At the end of the last MRI session (24 h post-MCAo), the animals were euthanized under profound anesthesia.

2.5 - Data processing

In-house macros built on the ImageJ software were used for data processing. PET images were reconstructed by the iterative OSEM-2D algorithm (resolution: 0.8x0.8x0.8mm). The quantified tissue activity concentration (kBq/ml) was divided by the injected activity in kBq/gram of body weight to give a Standardized Uptake Value (SUV, g/ml).

Time to Peak (TTP) was obtained from the first pass of the contrast agent P904® [19]. *Fractional* CBV maps (*f*CBV), were calculated as described in Valable and colleagues [20]. S_tO_2-MRI maps (in %) were computed from the equation published by Lemasson and collaborators [21]. Briefly, S_tO_2-MRI maps were calculated as a function of the T2* signal after correction of magnetic field inhomogeneities, total blood volume and T2 effects based on the following equation:

$S(t) = Ct * exp\ (-\frac{1}{T2}t\text{-}CBV.\gamma.\frac{4}{3}\pi.\ \Delta\chi_0.Hct(1 - S_tO_2\text{-}MRI)B_0.t)$, where Hct is the local hematocrit (set to 0.29), $\Delta\chi_0$ is the difference between the magnetic susceptibilities of fully oxygenated and fully deoxygenated hemoglobin (set to 0.264x106 (Centimeter–gram–second)), Ct is the proportionality constant.

Following spatial averaging of the T2*w EPI scans to attain a resolution of 0.3x0.3x1.5 mm in order to correct the macroscopic inhomogeneities, the T2*w EPI values were fitted pixelwise to the MR signal decay S(*t*) as a function of TE. T2 maps were obtained from a pixelwise fit to the MR signal decay measured from the four T2w EPI images acquired at TE= 40, 60, 80 and 100 ms. Voxels in which S_tO_2-*MRI* values were outside the range of 0-100 % were omitted.

All MRI scans were acquired such that the various MRI parameters were anatomically registered to each other. First, the X-ray scan (input) was registered by an automatic rigid way (normalized mutual information) on the T2-w MRI at 3h (reference) so as to obtain a registration matrix which was subsequently applied to the PET image. Following a visual inspection of brain contours, and whenever necessary, we manually refined the registration.

The lesion was clearly demarcated and therefore was manually delineated on each slice of ADC maps at 15min, 180min and 24 h post-MCAo. The hypoperfused areas were automatically defined on TTP maps. Voxels were considered abnormally perfused when the TTP value was superior to that of the mean contralateral tissue plus two standard deviations (SD). The penumbra

was defined as the region that displayed a significant perfusion deficit on TTP maps but normal ADC values (Figure 2A). The contralateral hemisphere, the ADC lesion and the penumbra were then used as masks and transferred onto all other modalities. Hypoxic tissue volumes were automatically segmented on [^{18}F]FMISO-PET images and corresponded to voxels with SUV values greater than the mean plus four SD of the contralateral hemisphere according to Spratt and colleagues [22], several thresholds have been tested and the four SD threshold provided the closest matching to manual outlines. Regions with a significant oxygen desaturation were defined on S_tO_2-MRI and corresponded to voxels with values less than the mean S_tO_2 values of the contralateral hemisphere minus two SD. This threshold allowed to delineate the area which, visually, exhibits a clear reduction in S_tO_2 values.

2.6 – Statistical analysis

Data are represented as mean ± standard error of the mean. Using JMP 12 software (SAS-Institute Inc, USA), statistical analyses were performed with ANOVA followed, where appropriate, by Tukey's post-hoc test, or with mixed model ANOVA with single random effect. Receiver-operating characteristic (ROC) curves were generated with JMP 12. Correlations analyses were performed by Pearson's test. Dice similarity coefficient was calculated following the formula: 2*intersect(A,B)/(absolute(A)+absolute(B)), where A: abnormal MRI signal and B: abnormal PET signal.

3 - RESULTS

Of the twelve rats, 2 died during the night following MCAo and thus were not examined at the last MRI session (24h). One rat was excluded from the analyses because of a hardly detectable lesion, probably due to a spontaneous reperfusion. The final sample size was then 11 for PET and MRI examinations at 3h, and 9 for the MRI examination performed at 24h.

3.1 - MRI findings

At 15 min after MCAo, a decrease in ADC values was observed primarily in subcortical structures. The ADC values were $9.0.10^{-4} \pm 0.6.10^{-4}$ and $5.3.10^{-4} \pm 0.1^{-4}$ mm^2/s in the contralateral tissue and lesion respectively ($p<0.0001$, *t*-test). At this time, tissue volume demonstrating a significantly reduced ADC was 72.2±17.7 mm^3 and further evolved at 3 hours to 126.3±25.4 mm^3 (Figure 2B). The lesion expanded even further during the following 24 h to reach a volume of 319.5±54.1 mm^3 (Figures 2A and 2B).

PWI performed 3h after MCAo revealed a greater volume of hypoperfused tissue (TTP-defined volume: 294.8±19.6 mm^3) in comparison to the volume which displayed a reduced ADC (Figure 2A; Figure 2C). The volume of PWI/DWI mismatch was 165.1±20.1 mm^3 (Figure 2A, Figure 2C). TTP values in such-defined penumbra were, as expected, higher in comparison to those measured within the contralateral hemisphere (15.5±2.8 s and 3.5±0.3 s respectively, $p<0.001$), but were significantly lower than those of the ADC-defined lesion (15.5±2.8 s versus 25.5±3.2 s, $p=<0.001$) (Figure 3A).

*f*CBV values were lower in the ADC-defined lesion in comparison to those of the contralateral hemisphere (2.79±0.30 % and 4.32±0.30 % respectively, $p=<0.001$). The penumbra displayed intermediate values of *f*CBV (3.49±0.30 %, significantly different from lesion and contralateral hemisphere, $p<0.05$) (Figure 3B).

S_tO_2-MRI maps revealed a reduced oxygen saturation in the ipsilateral hemisphere. The volume of tissue with a significant decrease in S_tO_2-MRI values was 242.0±22.9 mm^3 at 3h following MCAo (Figures 2A, 2C). Interestingly, the values of S_tO_2-MRI in the penumbra were significantly higher than those quantified in the core of ischemia, and significantly inferior to those in the

contralateral hemisphere (43.3±1.9 %, 52.3±2.0 % and 67.9±1.4 % respectively in the core, penumbra and contralateral hemisphere; $p<0.001$) (Figure 3C).

3.2 - PET findings

At 3h following MCAo, PET examinations revealed an increased [^{18}F]FMISO uptake in the affected hemisphere (Figure 2A). The volume of tissue with increased [^{18}F]FMISO uptake was 272.0±28.0 mm^3 (Figure 2C). [^{18}F]FMISO uptake was greater in the ADC-defined lesion when compared to the penumbra and to the contralateral hemisphere (1.33±0.09, 1.06±0.06 and 0.67±0.05 g/ml, respectively $p<0.01$ and $p<0.001$) (Figure 3D). Of note, the uptake of [^{18}F]FMISO in the penumbra was also significantly greater than the contralateral hemisphere ($p<0.001$, Figure 3D).

3.3 - S_tO_2-MRI threshold values

To evaluate the performance of S_tO_2-MRI to discriminate the penumbra from the healthy tissue, we employed ROC curve analysis. The area under the curve (AUC) value for S_tO_2-MRI, indicative of the best detection of the penumbra, was 0.983 (Figure 4A). A threshold value of 60% of S_tO_2-MRI (i.e. Youden index), with 91% specificity and 100% sensitivity, was derived from this analysis (Figure 4B). Based on the same analytical approach, an AUC value of 0.843 was found when the penumbra was compared to the ADC-defined lesion (Figure 4A). A threshold of 45% of oxygen saturation best discriminates these two compartments (72.7% specificity and 81.8% sensitivity) (Figure 4B). Remarkably, the ability of S_tO_2-MRI to differentiate the ischemic penumbra was similar to that of [^{18}F]FMISO–PET (Figure 4A).

3.4 - Comparisons between S_tO_2-MRI and [^{18}F]FMISO-PET

Figure 5 presents images of S_tO_2-MRI, [^{18}F]-FMISO-PET and the superimposition of both abnormalities on ADC image for each animal. The analysis of the overlap between increased uptake of [^{18}F]FMISO and low S_tO_2-MRI provided a Dice similarity coefficient of 0.61±0.1. Moreover, the volume of tissue with increased uptake of [^{18}F]FMISO was comparable to that with low S_tO_2-MRI (Figure 2C). There was a significant correlation between the volumes of these so-defined compartments (r=0.706; p=0.015) (Figure 6A). Furthermore, S_tO_2-MRI and [^{18}F]FMISO-PET-defined volumes (*i.e.* tissue with reduced oxygen saturation and tissue with increased [^{18}F]FMISO uptake, respectively), but not that defined on TTP maps (*i.e.* tissue with reduced perfusion), correlated with the final lesion (r=0.964, p<0.0001; r=0.870, p=0.002 and r=0.499, p=0.178, respectively) (Figure 6B).

4 - DISCUSSION

Based on a comparison with [^{18}F]FMISO-PET performed in the same animals, we validate the ability of MRI-based imaging of brain oxygen saturation (S_tO_2-MRI) to map hypoxia following acute stroke and to predict the final lesion volume.

Tissue volumes with decreased S_tO_2-MRI overlap and correlate with tissue volumes that display a significant uptake of [^{18}F]FMISO. These findings demonstrate that S_tO_2-MRI can delineate hypoxic tissue in the acute phase of stroke. Interestingly, the extent of the S_tO_2-MRI-defined hypoxia, but not the MRI-defined volume of hypoperfused tissue, predicts the extent of the final lesion as quantified with MRI 24 h following the occlusion. This prognostic capacity makes S_tO_2-MRI a valuable approach in the acute phase of stroke to map the tissue that will be irreversibly damaged, at least in situations with permanent arterial occlusion.

Over recent years, several reports have been published to show the potential of BOLD-based approaches to image brain oxygenation in laboratory animals and in man. The studies were performed both in conditions in which gas challenges were applied and also in pathological situations, such as acute stroke, in which hypoxia is the major hallmark [10,11,17]. Nonetheless, a formal validation of these imaging approaches with the PET-based reference standard techniques has not been attempted, except in two studies that compared T2*-MRI with FMISO-PET following stroke [23,24]. An updated version of qBOLD, termed mqBOLD, was developed. It takes into account estimates of T2, T2* and blood volume fraction [12,13,25]. The mqBOLD method is independent of any specific MRI sequence enabling a wide-spread and ready dissemination.

Based on the mqBOLD paradigm, Christen and colleagues [13] showed that S_tO_2-MRI was sensitive to changes in brain oxygenation under conditions of mild and severe hypoxia induced by decreases in the fraction of inspired oxygen and following diffuse brain traumatic injury and stroke. Similarly, in studies in which animals were subjected to different levels of hypoxia by changing F_iO_2 or in models of brain tumors, we showed that S_tO_2-MRI was able to detect both moderate and severe hypoxia while [^{18}F]FMISO PET and pimonidazole staining were sensitive to only severe hypoxia [26].

To further analyse the ability of S_tO_2-MRI to identify the heterogeneity of ischemic tissue, we employed the perfusion/diffusion mismatch paradigm to demarcate the early lesion along with the penumbra. In accordance with previous publications [9,13,27], the tissue S_tO_2 values in the contralateral hemisphere were 68% in average. Nevertheless, the ADC lesion displayed a more pronounced decrease in S_tO_2-MRI (43%) indicative of a severe hypoxia in this compromised compartment which may underlie the decrease in cerebral metabolic rate of oxygen ($CMRO_2$) observed in subjects with acute stroke [28,29]. The penumbra, with a relatively preserved blood

flow, as evidenced by measurements of TTP, was also characterized by an oxygen desaturation (52%) in comparison to the contralateral hemisphere, but to a level superior to that quantified in the ADC lesion. Interestingly, as the volume of tissue with decreased S_tO_2-MRI was lesser than that defined on TTP imaging, one may suggest that S_tO_2-MRI did not include benign oligemia. The profile of compartment-dependent decrease in oxygen saturation concords with that highlighted by [^{18}F]FMISO-PET imaging. The penumbra displayed an increase in [^{18}F]FMISO concentration relative to the contralateral hemisphere, signalling the hypoxic nature of that region as reported by Alawneh and colleagues [30]. In agreement with our studies, [^{18}F]FMISO retention was also observed in the core of the lesion which would imply that the cells in this region preserve a sufficient activity of the enzyme, nitroreductase, for the reduction and accumulation of [^{18}F]FMISO over the period of examination [6,31]. Whatever the mechanisms underlying [^{18}F]FMISO uptake in the different compartments of the ischemic tissue, our data underscore the equivalent profiles of decreased S_tO_2-MRI and increased [^{18}F]FMISO-PET signal in the core and the penumbra.

To further understand the interest of S_tO_2-MRI in discriminating different pathological compartments, we employed the threshold-independent receiver-operating characteristic (ROC) curve analysis approach. We found that the penumbra is discriminated from the healthy tissue with a threshold value of S_tO_2-MRI at 60% and with an AUC value near to unity (0.983 with 91% specificity and 100% sensitivity). These findings clearly show that S_tO_2-MRI is highly sensitive in the definition of the ischemic penumbra. This imaging paradigm also enables one, although with relatively less robustness, to distinguish between the core and the penumbra. A threshold value of tissue oxygen saturation of 45 % was established as the optimum to discriminate between the ADC-lesion and the vulnerable tissue (AUC value of 0.843 with 73 % specificity and 82 %

sensitivity). This cut-off value is near-identical to the 40% value reported by Christen and colleagues in rats subjected to MCAo [13]. However, in man, these S_tO_2-MRI thresholds could vary, since blood oxygen dissociation curves differ between man and rat [32]. In our studies, the ROC analyses revealed that S_tO_2-MRI can map the different pathophysiological compartments (*viz*. core, penumbra) with the same diagnostic capacity as those obtained with [^{18}F]FMISO-PET. Again, this similarity argues for the strength of the S_tO_2-MRI as an imaging modality which merits to be implemented in clinical studies: to better characterize the pathophysiology of brain tissue following stroke; to develop its reproducibility and its robustness in the frame of multicenter trials; and, *in fine*, to improve patient care.

There are some limitations in our study. First, all imaging parameters (StO_2-MRI and [^{18}F]FMISO-PET) are compared to the DW-MRI abnormalities. We did not perform histological confirmation of the actual size of the lesion in the late phase. Second, EPI acquisitions unfortunately cause deformations on images which makes it more difficult to compare the different markers, but these deformations are located very mainly where there is no lesion.

5 - CONCLUSION

The data gathered in the present study clearly show that S_tO_2-MRI is able to image the heterogeneous profile of brain tissue in the acute phase of stroke and to predict the final lesion. Given the straightforwardness of this imaging modality and the fact it does not require any additional examination for the patients, it should be considered as a component of an MRI examination in acute stroke patients.

Acknowledgements

This study was supported in part by the Centre National de la Recherche Scientifique (CNRS), the Université de Caen-Normandie (UCN), the Conseil Régional de Normandie, the

Fondation Elen, the European Union-Fonds de Développement Régional (FEDER), L'Europe s'engage en Basse-Normandie, the National Agency for Research (ANR IMOXY "ANR- 11-BSV5-004") and the National Agency for Research "Investissements d'Avenir" (Labex IRON, ANR-11-LABEX-0018-01). The authors wish to thank the personnel of Cyceron and the CURB for their technical support.

References

1.Astrup J, Siesjö BK, Symon L. Thresholds in cerebral ischemia - the ischemic penumbra. Stroke. 1981;12:723–25.

2. Markus M, Reutens DC, Kazui S, Read S, Wright P, Pearce DC, et al. Hypoxic tissue in ischaemic stroke: persistence and clinical consequences of spontaneous survival. Brain. 2004;127:1427–46.

3. Mies G, Ishimaru S, Xie Y, Seo K, Hossmann KA. Ischemic thresholds of cerebral protein synthesis and energy state following middle cerebral artery occlusion in rat. J Cereb Blood Flow Metab. 1991;11:753–61.

4. Davis S, Donnan GA. Time is Penumbra: imaging, selection and outcome. The Johann jacob wepfer award 2014. Cerebrovasc Dis. 2014;38:59–72.

5. Read SJ, Hirano T, Abbott DF, Markus R, Sachinidis JI, Tochon-Danguy HJ, et al. The fate of hypoxic tissue on ^{18}F-fluoromisonidazole positron emission tomography after ischemic stroke. Ann Neurol. 2000;48:228–35.

6. Takasawa M, Moustafa RR, Baron J-C. Applications of nitroimidazole in vivo hypoxia imaging in ischemic stroke. Stroke. 2008;39:1629–37.

7. Takasawa M, Beech JS, Fryer TD, Hong YT, Hughes JL, Igase K, et al. Imaging of brain hypoxia in permanent and temporary middle cerebral artery occlusion in the rat using ^{18}F-fluoromisonidazole and positron emission tomography: a pilot study. J Cereb Blood Flow Metab. 2007 27:679-89.

8. Williamson DJ, Ejaz S, Sitnikov S, Fryer TD, Sawiak SJ, Burke P, et al. A comparison of four PET tracers for brain hypoxia mapping in a rodent model of stroke. Nucl Med Biol. 2013;40:338–44.

9. An H, Liu Q, Chen Y, Lin W. Evaluation of MR-derived cerebral oxygen metabolic index in experimental hyperoxic hypercapnia, hypoxia, and ischemia. Stroke. 2009;40:2165–72.

10. Jensen-Kondering U, Baron J-C. Oxygen imaging by MRI: can blood oxygen level-dependent imaging depict the ischemic penumbra? Stroke. 2012;43:2264–69.

11. An H, Ford AL, Vo KD, Liu Q, Chen Y, Lee JM, et al. Imaging Oxygen Metabolism In Acute Stroke Using MRI. Curr Radiol Rep. 2014;2:39.

12. Christen T, Lemasson B, Pannetier N, Farion R, Segebarth C, Rémy C, et al. Evaluation of a quantitative blood oxygenation level-dependent (qBOLD) approach to map local blood oxygen saturation. NMR Biomed. 2011;24:393–403.

13. Christen T, Bouzat P, Pannetier N, Coquery N, Moisan A, Lemasson B, et al. Tissue oxygen saturation mapping with magnetic resonance imaging. J Cereb Blood Flow Metab. 2014;34:1550–57.

14. He X, Yablonskiy DA. Quantitative BOLD: mapping of human cerebral deoxygenated blood volume and oxygen extraction fraction: default state. Magn Reson Med. 2007;57:115–26.

15. Bouvier J, Detante O, Tahon F, Attye A, Perret T, Chechin D, et al. Reduced $CMRO_2$ and cerebrovascular reserve in patients with severe intracranial arterial stenosis: a combined multiparametric qBOLD oxygenation and BOLD fMRI study. Hum Brain Mapp. 2015;36:695–706.

16. Corroyer-Dulmont A, Chakhoyan A, Collet S, Durand L, MacKenzie EL, Petit E, et al. Imaging Modalities to Assess Oxygen Status in Glioblastoma. Front Med (Lausanne). 2015;2:57.

17. Boisserand LS, Lemasson B, Hirschler L, Moisan A, Hubert V, Barbier EL, et al. Multiparametric magnetic resonance imaging including oxygenation mapping of experimental ischaemic stroke. J Cereb Blood Flow Metab. 2017; 37:2196-207.

18. Quittet MS, Touzani O, Sindji L, Cayon J, Fillesoye F, Toutain J, et al. Effects of mesenchymal stem cell therapy, in association with pharmacologically active microcarriers releasing VEGF, in an ischaemic stroke model in the rat. Acta Biomater. 2015;15:77–88.

19. Letourneur A, Roussel S, Toutain J, Bernaudin M, Touzani O. Impact of genetic and renovascular chronic arterial hypertension on the acute spatiotemporal evolution of the ischemic penumbra: a sequential study with MRI in the rat. J Cereb Blood Flow Metab. 2011;31:504–13.

20. Valable S, Lemasson B, Farion R, Beaumont M, Segebarth C, Remy C, et al. Assessment of blood volume, vessel size, and the expression of angiogenic factors in two rat glioma models: a longitudinal in vivo and ex vivo study. NMR Biomed. 2008;21:1043–56.

21. Lemasson B, Christen T, Serduc R, Maisin C, Bouchet A, LeDuc G, et al. Evaluation of the relationship between MR estimates of blood oxygen saturation and hypoxia: effect of an antiangiogenic treatment on a gliosarcoma model. Radiology. 2012;265:743–52.

22. Spratt NJ, Donnan GA, McLeod DD, Howells DW. “Salvaged” stroke ischaemic penumbra shows significant injury: studies with the hypoxia tracer FMISO. J Cereb Blood Flow Metab. 2011;31:934–43.

23. Donswijk ML, Jones PS, Guadagno JV, et al. T2*-weighted MRI versus oxygen extraction fraction PET in acute stroke. Cerebrovasc Dis. 2009;28:306–13.

24. Jensen-Kondering U, Manavaki R, Ejaz S, Sawiak SJ, Carpenter TA, Fryer TD, et al.Brain hypoxia mapping in acute stroke: Back-to-back T2' MR versus (^{18})F-fluoromisonidazole PET in rodents. Int J Stroke 2017; 12:752-60.

25. Christen T, Lemasson B, Pannetier N, Farion R, Remy C, Zaharchuk G, et al. Is T2* enough to assess oxygenation? Quantitative blood oxygen level-dependent analysis in brain tumor. Radiology. 2012;262:495–502.

26. Valable S, Corroyer-Dulmont A, Chakhoyan A, Durand L, Toutain J, Divoux D, et al. Imaging of brain oxygenation with magnetic resonance imaging: A validation with positron emission tomography in the healthy and tumoural brain. J Cereb Blood Flow Metab. 2016;37:2584–97.

27. He X, Zhu M, Yablonskiy DA. Validation of oxygen extraction fraction measurement by qBOLD technique. Magn Reson Med. 2008;60:882–88.

28. Touzani O, Young AR, Derlon JM, Beaudouin V, Marchal G, Rioux P, et al. Sequential studies of severely hypometabolic tissue volumes after permanent middle cerebral artery occlusion. A positron emission tomographic investigation in anesthetized baboons. Stroke. 1995;26:2112-19.

29. Gersing AS, Ankenbrank M, Schwaiger BJ, Toth V, Janssen I, Kooijman H, et al. Mapping of cerebral metabolic rate of oxygen using dynamic susceptibility contrast and blood oxygen level dependent MR imaging in acute ischemic stroke. Neuroradiology. 2015;57:1253–61.

30. Alawneh JA, Moustafa RR, Marrapu ST, Jensen-Kondering U, Morris RS, Jones PS, et al. Diffusion and perfusion correlates of the ^{18}F-MISO PET lesion in acute stroke: pilot study. Eur J Nucl Med Mol Imaging. 2014;41:736–44.

31. Rojas S, Herance JR, Abad S, Jiménez X, Pareto D, Ruiz A, et al. Evaluation of hypoxic tissue dynamics with ^{18}F-FMISO PET in a rat model of permanent cerebral ischemia. Mol Imaging Biol. 2011;13:558–64.

32. Schmidt-Nielsen K. Energy metabolism, body size, and problems of scaling. *Fed Proc*. 1970;29:1524–32.

Figure 1

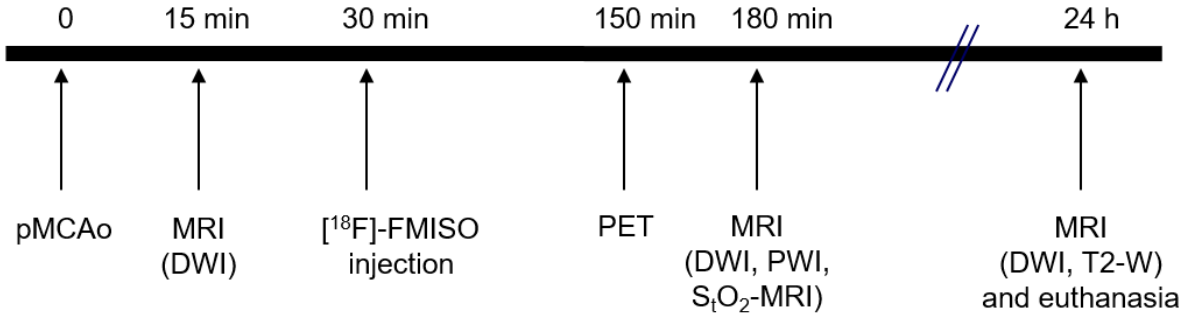

Figure 1. Experimental protocol: each rat was subjected to permanent middle cerebral artery occlusion (pMCAo), then to sequential magnetic resonance imaging (MRI) and positron emission tomography (PET) examinations. DWI: diffusion-weighted imaging, PWI: perfusion-weighted imaging, S_tO_2-MRI: Brain tissue oxygen saturation, T2-WI: T2-weighted MR imaging, [^{18}F]-FMISO: 18-fluorine-fluoromisonidazole.

Figure 2

A

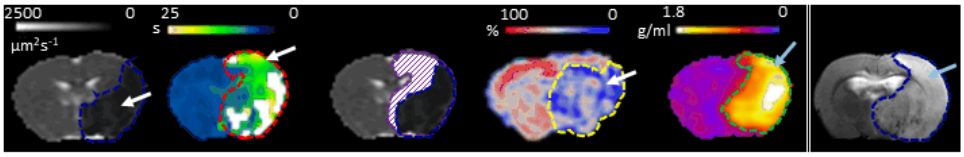

ADC Time-To-Peak Penumbra S_tO_2-MRI [^{18}F]-FMISO-PET T2w at 24h

B

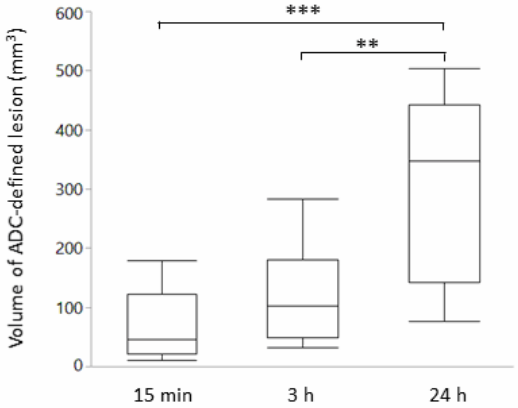

C

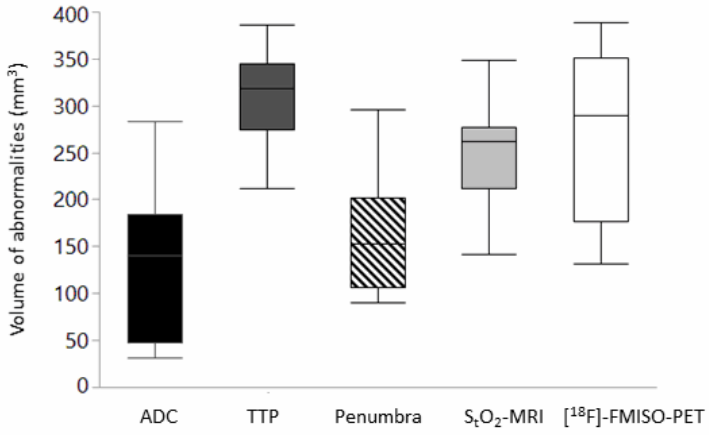

Figure 2: **(A)** Representative images obtained in one rat at 3h following MCAo. Apparent diffusion coefficient (ADC) map depicts the core of ischemia (arrow). Time-to-peak (TTP) map reveals a larger zone of hypoperfusion (arrow). The penumbra was delineated as the mismatch between perfusion and diffusion abnormalities (hatched purple). The S_tO_2-MRI map shows the area with reduced oxygen saturation (arrow). [^{18}F]-FMISO-PET delineates the hypoxic area with increased retention of [^{18}F]-FMISO (arrow). The T2-WI, acquired 24 h after MCA occlusion, shows the consolidated lesion (arrow).

(B) Evolution of ADC-defined lesion volumes. The lesion demonstrable at 15min, expanded at 3h, and even more so at 24h following MCAo.**, ***$p<0.01$, $p<0.001$ respectively; ANOVA with repeated measures followed by Tukey's post-hoc test. The boxes define the interquartile range; the solid horizontal line the median and the whiskers represent the minimal and maximal values.

(C) Volumes of brain compartments at 3h following MCAo. Time-to-peak (TTP): tissue volume with decreased perfusion; Penumbra: tissue with PWI/DWI mismatch; S_tO_2-MRI: tissue that displays a decrease in oxygen saturation, [^{18}F]-FMISO-PET: tissue volume that shows an increased retention of [^{18}F]-FMISO. The boxes define the interquartile range; the solid horizontal line the median and the whiskers represent the minimal and maximal values.

Figure 3

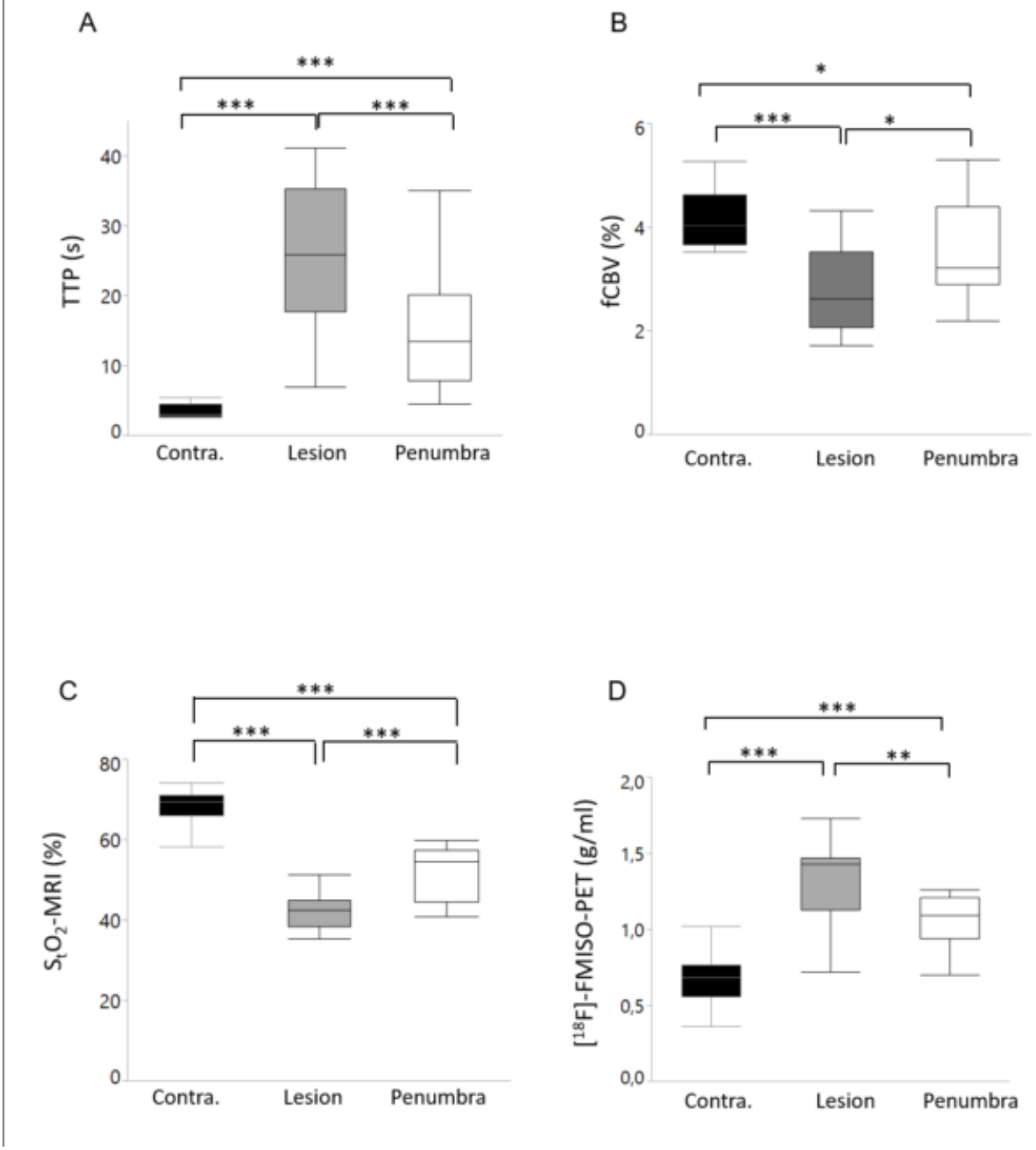

Figure 3. Values of time-to-peak (TTP) in seconds **(A)**, fractional cerebral blood volume (*f*CBV) in % **(B)**, tissue oxygen saturation (S_tO_2-MRI) in % **(C)** and [^{18}F]-FMISO-PET uptake in g/ml **(D)** in the contralateral hemisphere (contra.), the lesion core (lesion) and the penumbra. *, **, ***p<0.05, 0.01, 0.001 respectively, mixed model ANOVA with single random effect (the

animal being the random variable. The boxes define the interquartile range; the solid horizontal line the median and the whiskers represent the minimal and maximal values.

Figure 4

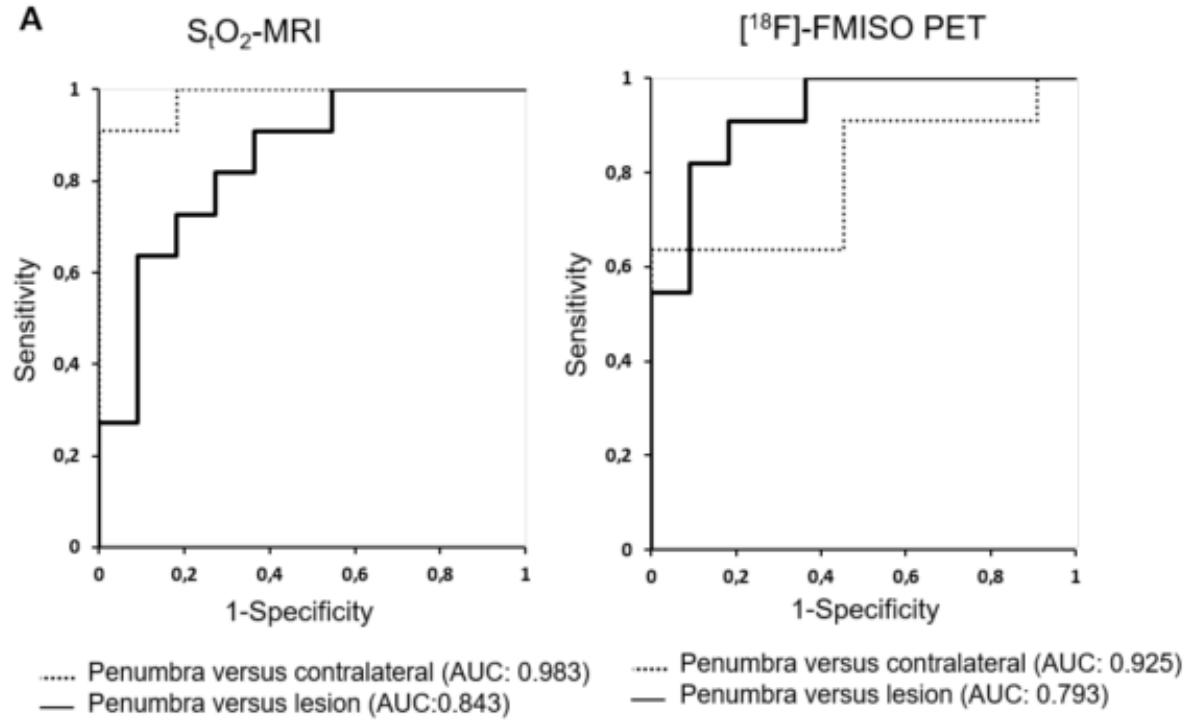
A
StO2-MRI
[18F]-FMISO PET
Sensitivity
1-Specificity
0
0,2
0,4
0,6
0,8
1
..... Penumbra versus contralateral (AUC: 0.983)
— Penumbra versus lesion (AUC:0.843)
..... Penumbra versus contralateral (AUC: 0.925)
— Penumbra versus lesion (AUC: 0.793)

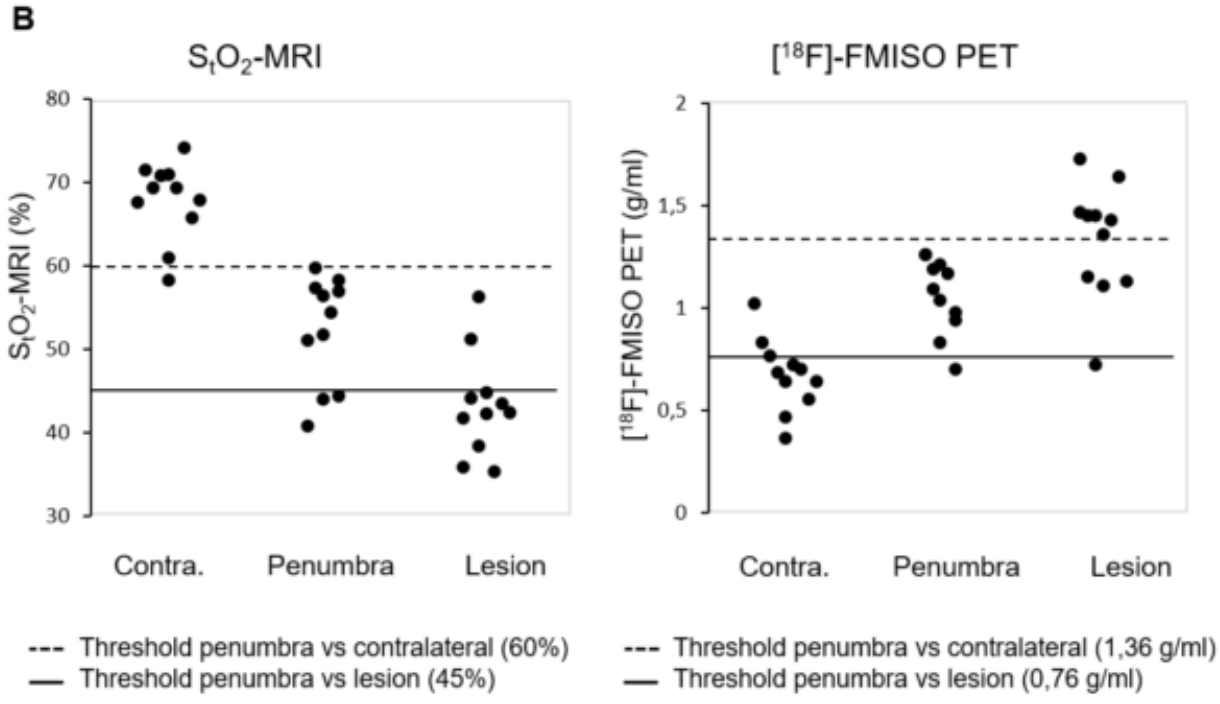
B
StO2-MRI
[18F]-FMISO PET
StO2-MRI (%)
[18F]-FMISO PET (g/ml)
80
70
60
50
40
30
2
1,5
1
0,5
0
Contra.
Penumbra
Lesion
--- Threshold penumbra vs contralateral (60%)
— Threshold penumbra vs lesion (45%)
--- Threshold penumbra vs contralateral (1,36 g/ml)
— Threshold penumbra vs lesion (0,76 g/ml)

Figure 4. (A): Receiver-operating characteristic (ROC) illustrating the capacity of S_tO_2-MRI and [^{18}F]-FMISO-PET to discriminate the penumbra from the contralateral healthy hemisphere (dashed line) and the penumbra from the core of the lesion (solid line). The ROC curve analysis was performed for all animals based on S_tO_2-MRI and [^{18}F]-FMISO-PET values quantified in the contralateral hemisphere, penumbra and the lesion. AUC: area under the curve.

(B) ROC analysis-derived thresholds of S_tO_2-MRI (in %) and [^{18}F]-FMISO-PET (in g/ml) that distinguish the contralateral tissue (contra.) from the penumbra (dashed line) and the penumbra from the lesion (solid line). Each rat is represented by a filled circle.

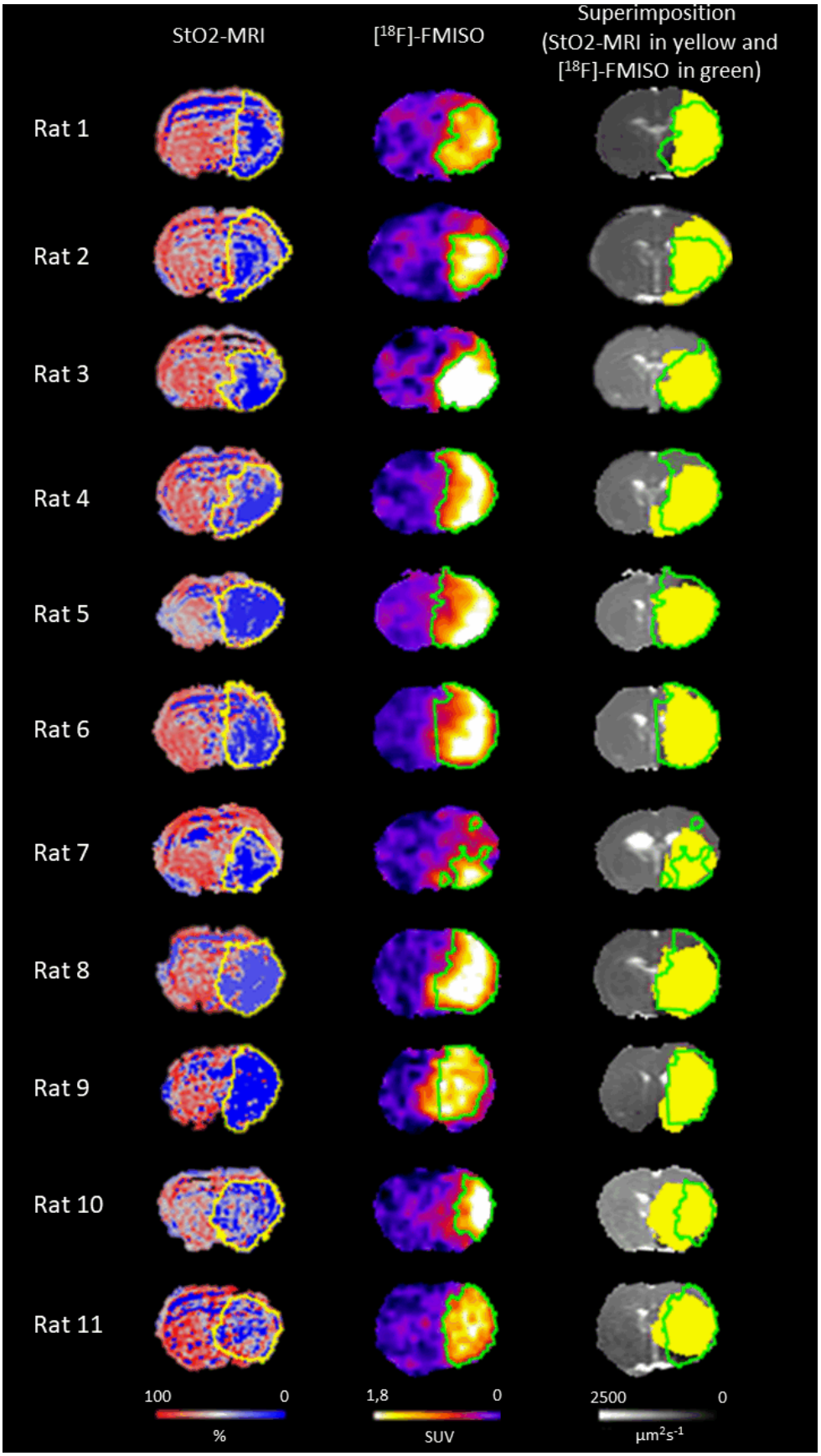
StO2-MRI
[18F]-FMISO
Superimposition
(StO2-MRI in yellow and
[18F]-FMISO in green)
Rat 1
Rat 2
Rat 3
Rat 4
Rat 5
Rat 6
Rat 7
Rat 8
Rat 9
Rat 10
Rat 11
100
0
%
1,8
0
SUV
2500
0
µm²s⁻¹

Figure 5. Representative images of S_tO_2-MRI, [^{18}F]-FMISO-PET and the superimposition of both abnormalities on ADC image for each animal. S_tO_2-MRI abnormality is delinated in yellow and [^{18}F]-FMISO-PET abnormality in green.

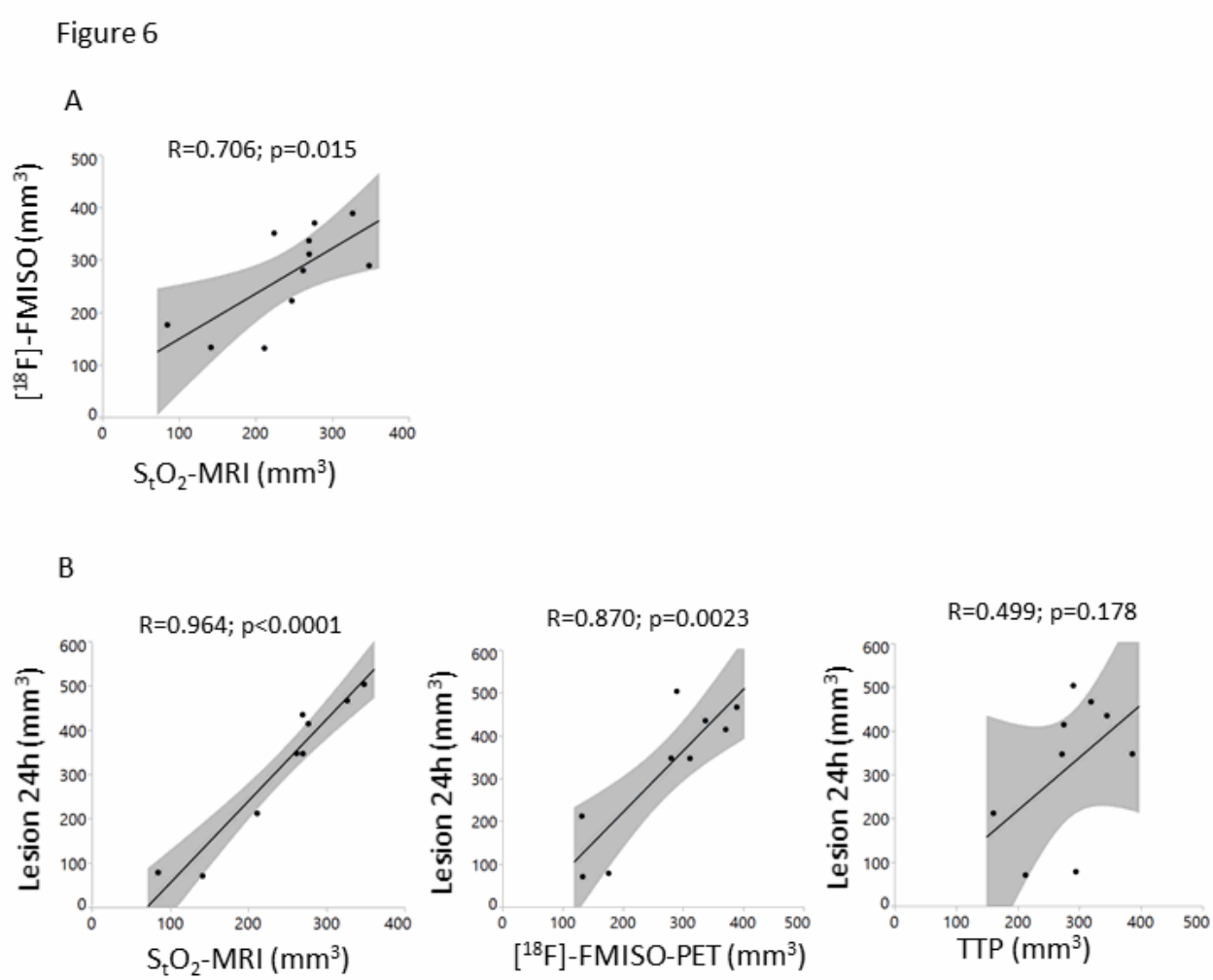

Figure 6. **(A)** Cross-correlation between hypoxic volumes defined on S_tO_2-MRI and on [^{18}F]-FMISO-PET. Grey shadings are the 95% confidence intervals.

(B) Correlations of oxygen saturation-defined (S_tO_2-MRI), [^{18}F]-FMISO-PET-defined, and TTP-defined volumes determined 3h after MCAo as function of the final lesion volume measured on T2-w-MRI 24h after ischemia. Grey shadings indicate the 95% confidence intervals.